European Journal of Immunology
Clinical·Basic·Translational

Immunity to infection

Basic

Research Article

Enolase 1 of *Candida albicans* binds human CD4$^+$ T cells and modulates naïve and memory responses

Muhammad Daud[1], Prasad Dasari[2], Marion Adelfinger[3], Daniela Langenhorst[1], Jasmin Lother[3], Dragana Slavkovic-Lukic[3], Carsten Berges[3], Michaela Kruhm[3], Annette Galler[4], Cathrin Schleussner[4], Christian H. Luther[5], Karl Alberter[1], Anton Althammer[1], Haroon Shaikh[3], Niklas Pallmann[1], Jochen Bodem[1], Mohammed El-Mowafy[1,6], Andreas Beilhack[3], Marcus Dittrich[5,7], Max S. Topp[3], Peter F. Zipfel[#2,8] and Niklas Beyersdorf[#1]

[1] Institute for Virology and Immunobiology, University of Würzburg, Würzburg, Germany
[2] Leibniz Institute for Natural Product Research and Infection Biology, Hans-Knöll-Institute, Jena, Germany
[3] Department of Internal Medicine II, Division of Hematology, University Hospital Würzburg, Würzburg, Germany
[4] T-Balance Therapeutics, Frankfurt, Germany
[5] Chair of Bioinformatics, University of Würzburg, Würzburg, Germany
[6] Faculty of Pharmacy, Department of Microbiology & Immunology, Mansoura University, Mansoura, Egypt
[7] Institute of Human Genetics, University of Würzburg, Würzburg, Germany
[8] Friedrich Schiller University, Jena, Germany

To obtain a better understanding of the biology behind life-threatening fungal infections caused by *Candida albicans*, we recently conducted an in silico screening for fungal and host protein interaction partners. We report here that the extracellular domain of human CD4 binds to the moonlighting protein enolase 1 (Eno1) of *C. albicans* as predicted bioinformatically. By using different anti-CD4 monoclonal antibodies, we determined that *C. albicans* Eno1 (CaEno1) primarily binds to the extracellular domain 3 of CD4. Functionally, we observed that CaEno1 binding to CD4 activated lymphocyte-specific protein tyrosine kinase (LCK), which was also the case for anti-CD4 monoclonal antibodies tested in parallel. CaEno1 binding to naïve human CD4$^+$ T cells skewed cytokine secretion toward a Th2 profile indicative of poor fungal control. Moreover, CaEno1 inhibited human memory CD4$^+$ T-cell recall responses. Therapeutically, CD4$^+$ T cells transduced with a p41/Crf1-specific T-cell receptor developed for adoptive T-cell therapy were not inhibited by CaEno1 in vitro. Together, the interaction of human CD4$^+$ T cells with CaEno1 modulated host CD4$^+$ T-cell responses in favor of the fungus. Thus, CaEno1 mediates not only immune evasion through its interference with complement regulators but also through the direct modulation of CD4$^+$ T-cell responses.

Keywords: *Candida albicans* · Enolase 1 · Human CD4$^+$ T cells · Immune evasion · T-cell activation

Additional supporting information may be found online in the Supporting Information section at the end of the article.

Correspondence: Dr. Niklas Beyersdorf
e-mail: niklas.beyersdorf@vim.uni-wuerzburg.de

[#]These authors contributed equally to this work.

Introduction

A better understanding of the interactions of fungal pathogens with the human host will improve our overall understanding of fungal infection biology and will lead to better therapeutic options for invasive fungal disease (IFD). Protein–protein interactions are crucial to the interplay of host and fungal pathogens. As many of these interactions and their biological significance are still unknown, bioinformatical predictions identifying likely candidates are powerful tools to guide further wet-lab research into host–fungus interactions. Recently, the moonlighting protein enolase 1 from *Candida albicans* (CaEno1) has been predicted to interact with mouse [1] and human CD4 [2].

In humans, $CD4^+$ T cells and monocytes express CD4 levels that can be readily detected by flow cytometry [3]. On monocytes, CD4 functions as a receptor for IL-16 activating monocytes and driving chemotaxis [4–6]. In contrast, on $CD4^+$ T cells, the primary function of CD4 is to bind to human leukocyte antigen (HLA) class II molecules stabilizing the interaction of the T-cell receptor (TCR) with peptide/HLA class II molecules. Moreover, the immobilization of CD4 by HLA class II/peptide complexes contributes to T-cell activation by bringing the kinase LCK into the proximity of the TCR [7, 8]. Phosphorylation of Tyr505 by the C-terminal Src kinase leads to the binding of phospho-Tyr505 to the SH2 domain of LCK, that is, closing of the "latch," and the inhibition of LCK activity. Outside the immunological synapse, the phosphatase CD45 dephosphorylates Tyr505 of LCK, thus maintaining an open confirmation. Similar to the interaction of CD4 with HLA class II/peptide complexes, anti-CD4 monoclonal antibodies (mAb)-like clones RPA-T4 and tregalizumab have also been shown to induce LCK phosphorylation [9].

$CD4^+$ T cells crucially contribute to the control of fungal infections (reviewed in Ref. [10]). However, at the time point of the shift of *C. albicans* from harmless commensal to an invasive pathogen, preexisting T-cell immunity among different donors varies considerably [11], indicating that the host's immune response will be driven to varying degrees by memory and naïve $CD4^+$ T cells.

Eno1 belongs to a group of immune evasion proteins expressed by fungal pathogens like the yeast *C. albicans* and the mold *Aspergillus fumigatus* [12–19]. Importantly, these proteins mediate immune evasion by interfering with the complement system, the main humoral component of innate immunity.

Apart from interacting with innate immunity, fungal immune evasion proteins also interact with cells of adaptive immunity. Commensalism (*C. albicans*) and particularly occupational exposure (*A. fumigatus*) can induce class-switched antibody responses against many fungal immune evasion proteins, including Eno1 [20, 21]. As antibody class switching is greatly facilitated by helper $CD4^+$ T cells, it is not surprising that some fungal immune evasion proteins, most prominently Eno1, have been shown to also contain $CD4^+$ T-cell epitopes [21]. Recognition of immune evasion protein–derived antigens by $CD4^+$ T cells may, thus, critically contribute to immunopathology in patients with allergic bronchopulmonary aspergillosis [22]. However, here, fungal immune evasion proteins appear to differentially affect pathogenesis with Eno1 of *A. fumigatus* potently stimulating protective $CD4^+$ $Foxp3^+$ regulatory cell (Treg) and Aspf2 of *A. fumigatus* triggering effector $CD4^+$ T cells [23]. However, Aspf2-reactive T cells display an "exhausted" memory phenotype in healthy blood donors, that is, the lack of cytokine secretion, rendering them unlikely drivers of immunopathology [24].

Recently, we identified another level of interaction of fungal immune evasion proteins with the host's immune system. We observed that Pra1 of *C. albicans* could directly bind to human and mouse lymphocytes, that is, cells not expressing the known receptor of Pra1 CD11b/CD18. The binding of Pra1 was particularly efficient for Th1 cells in which the fungal protein suppressed the secretion of IFN-γ, thus inhibiting fungal clearance [25].

In this study, we analyzed the interaction of CaEno1 with human CD4 and human $CD4^+$ T cells. We found that CaEno1, indeed, binds to the extracellular part of human CD4. Moreover, the binding of CaEno1 to CD4 modulated cytokine secretion by naïve human T cells and interfered with antigenic recall responses of memory $CD4^+$ T cells.

Results

Eno1 binds to human CD4

Guided by the bioinformatical prediction that fungal Eno1 is a potential binding partner for human CD4 [1, 2], we established a FACS-based detection system to study this interaction. As a substrate for CaEno1 binding, we first immobilized the recombinant extracellular domain of human CD4 on Dynabeads (Supporting information Fig. 1) and then reacted the coated beads with CaEno1 (Fig. 1A and B). CaEno1 clearly bound to the CD4-coated beads confirming the bioinformatic prediction of molecular CaEno1 and human CD4 interaction. The same was true for Eno1 from *A. fumigatus* (AfEno1) (Supporting information Fig. 2) but not for human Eno1 (hEno1) (Supporting information Fig. 3).

Human CD4 consists of four different extracellular domains. To map the binding sites of CaEno1, we preincubated the Dynabeads with anti-CD4 mAb against domain 1 (RPA-T4), domain 2 (Tregalizumab), or domain 3 (OKT-4) [9, 26]. Only mAb OKT-4 reproducibly and dose-dependently inhibited CaEno1 binding to the CD4-coated Dynabeads (Fig. 1C–F). This suggests that CaEno1 binds extracellular domain 3, but not domains 1 and 2 of human CD4. In line with this, we observed that CaEno1 did not inhibit the infection of CD4-expressing MT4 and TZM cell line cells with NL4-3-derived T-tropic b-type or with MJ4-derived M-tropic c-type human immunodeficiency virus (HIV)-1 (Supporting information Fig. 4).

Binding of CaEno1 to human $CD4^+$ T cells induces LCK phosphorylation

Apart from stabilizing the interaction of the TCR with peptide/HLA class II molecules, CD4 plays a key role in T-cell

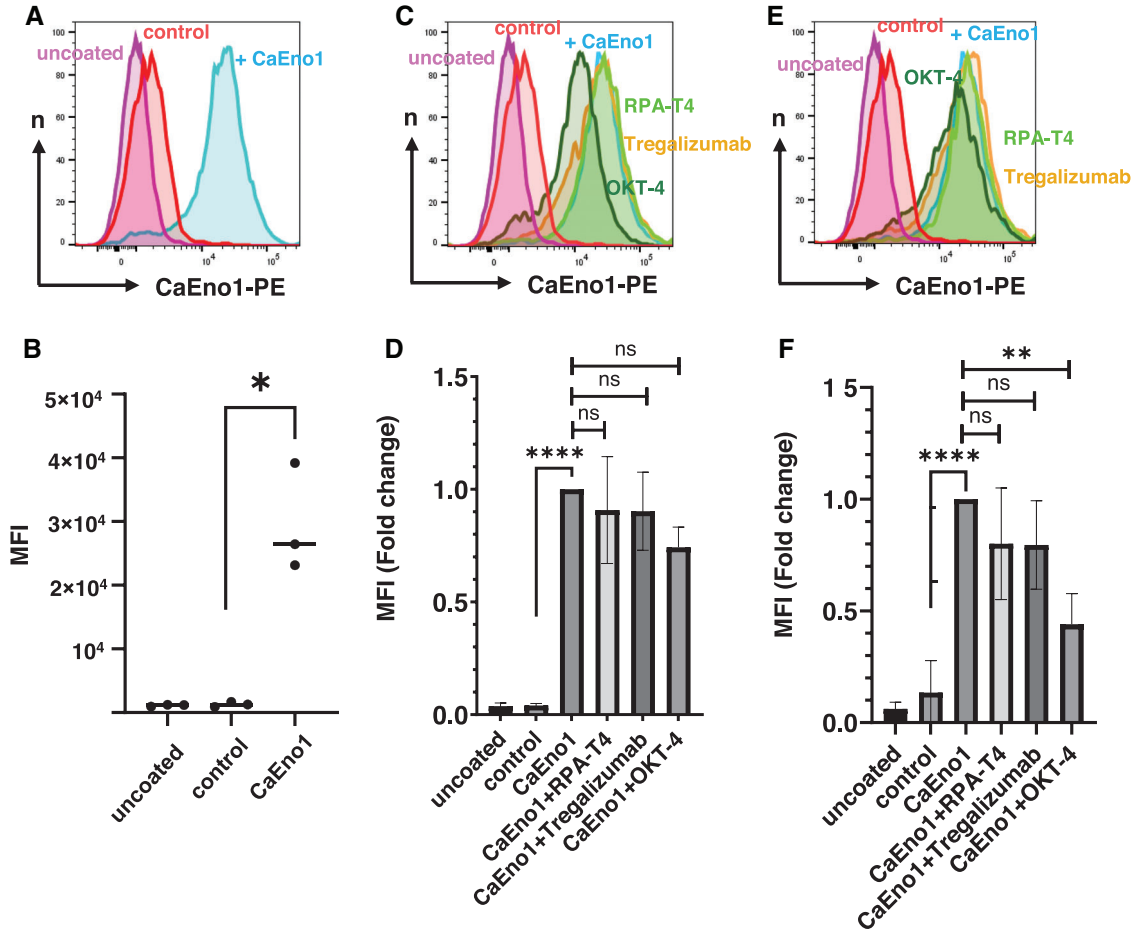

Figure 1. *Candida albicans* Eno1 (CaEno1) binds human CD4. Dynabeads M-270 Epoxy were coated with recombinant human CD4. (A) CaEno1 (1 μg/mL) was incubated with CD4-coated beads for 20 min at room temperature. The binding of CaEno1 to human CD4 was detected by indirect immunofluorescence (blue histogram). Negative control (control): No addition of CaEno1 (red histogram). Uncoated: Beads without CD4 coating but incubated with CaEno1 (pink histogram). (B) Median fluorescence intensities of CaEno1 binding to CD4 (n = 3 separate experiments). A paired one-tailed t-test was used to compare the values in the absence (control) and presence of CaEno1 (p-value <0.05 = significant). (C) Anti-CD4 monoclonal antibodies (mAb) at 1 μg/mL or (E) 10 μg/mL were used to inhibit binding of CaEno1 to CD4: RPA-T4 (light green), Tregalizumab (orange), and OKT-4 (dark green). Binding of CaEno1 to CD4 in the absence of mAb (blue, positive control) and the negative controls without CaEno1 (red) and uncoated beads reacted with CaEno1 (pink) are also shown. (A, C, and E) Representative results from a representative experiment of a total of three different experiments with similar results are shown. (D) The bar graph shows normalized data (MFI positive control = 1) of three independent experiments (n = 3) for 1 μg/mL and (F) 10 μg/mL of anti-CD4 mAb. (D and F) Each figure shows means ± SD. Values were tested with the one-way ANOVA followed by Dunnett's multiple comparisons test. Exact p-values for the indicated comparisons are shown. (p-Values <0.05 were regarded as being statistically significant.)

activation through activating LCK (reviewed in Refs. [8, 27]). Similar to the interaction of CD4 with HLA class II/peptide complexes, surface binding of anti-CD4 mAbs (e.g., clone RPA-T4 and OKT-4) to CD4 can induce LCK phosphorylation [9]. We, thus, asked whether the binding of CaEno1 to purified $CD4^+$ T cells would also induce the phosphorylation of LCK at Tyr505 and/or Tyr394. As positive controls, we used the anti-CD4 mAb RPA-T4 [9], anti-CD3 mAb [28], and H_2O_2 [29, 30]. Detection of phospho-Tyr505 and -Tyr394 by intracellular flow cytometry staining (Supporting information Fig. 5) revealed that CaEno1 induced phosphorylation of LCK at both sites (Fig. 2A–C). Thus, CaEno1 binding to $CD4^+$ T cells induced LCK phosphorylation as did anti-CD4 mAb RPA-T4 and the two other positive controls used.

CaEno1 skews cytokine secretion by activated naïve human $CD4^+$ T cells primarily toward Th2

During commensalism and in fungal disease, CaEno1 might shape T-cell immunity as it is the most abundantly expressed protein of *C. albicans* [31]. We, thus, analyzed the impact of CaEno1 on cytokine secretion by purified naïve human $CD4^+$ T cells (Supporting information Fig. 6A and B) co-stimulated with Dynabeads Human T-Activator CD3/CD28. Analyzing $CD4^+$ T cells from ten different healthy blood donors revealed that CaEno1 reduced IFN-γ secretion by $CD4^+$ T cells from eight donors (Fig. 3A), whereas increasing IL-5 secretion in six out of ten experiments (Fig. 3B). Together, this led to a Th2 bias (decreased ratio of IFN-γ over IL-5 secretion) in six and a Th1 bias in three out of ten experiments

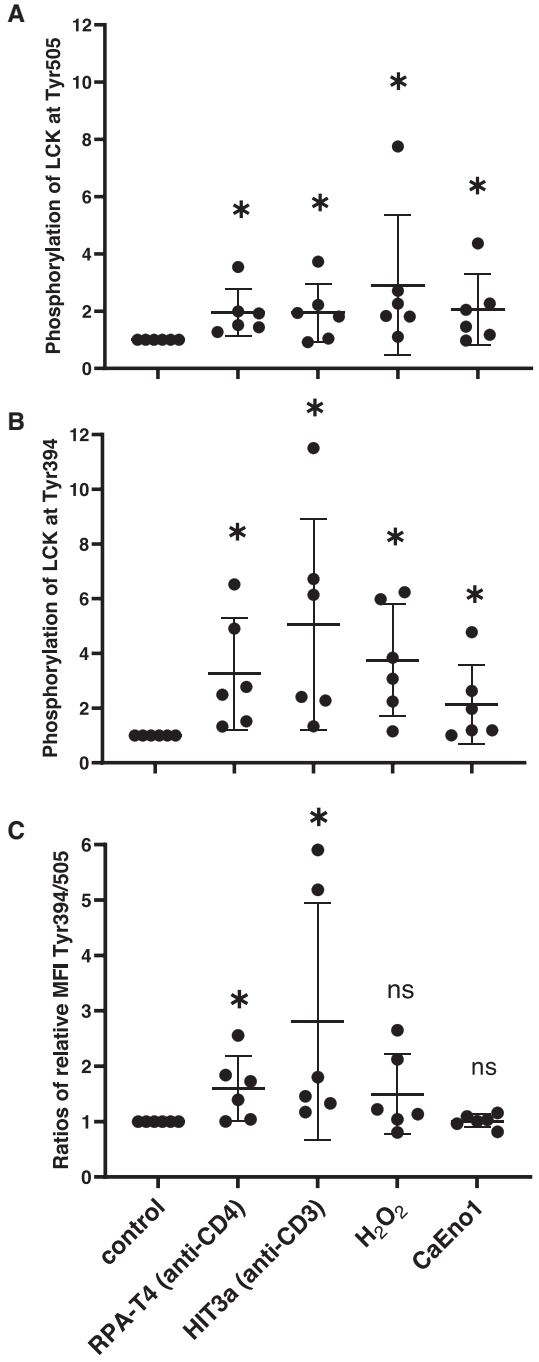

Figure 2. Binding of *Candida albicans* Eno1 (CaEno1) to CD4$^+$ T cells activates LCK. CD4$^+$ T cells were purified from peripheral blood mononuclear cells (PBMCs) of healthy donors (n = 6) and incubated with CaEno1 (1 μg/mL) at 37°C for 30 min. In parallel, CD4$^+$ T cells were incubated with anti-CD4 monoclonal antibodies (mAb) RPA-T4 (1 μg/mL), anti-CD3 mAb HIT3a (1 μg/mL), or H_2O_2 (5 mM). Purified CD4$^+$ T cells cultured in medium only were used as a negative control (control). The graphs summarize median fluorescence intensities for anti-phospho-LCK stainings: (A) Tyr505 and (B) Tyr394. The data were normalized to the negative control (MFI (control) = 1). (C) Ratios of the relative MFI for the phospho-Tyr394 over the phospho-Tyr505 stainings. (A–C) Means ± SD (n = 6 donors/experiments). A one-sided Wilcoxon signed-rank test was used to compare values to the negative control. Exact p-values for comparisons to the "control" group are shown. (p-Values <0.05 were regarded as being statistically significant.)

Table 1. Overview of proportion of donors responding to different recall antigens.

Recall Ag	Total no. of donors	No. of donor responded	Percent responders
PPD	43	28	65
Td	10	6	60
Candida albicans (MP65)	10	3	30
CMV	10	2	20
CaEno1	43	16	37
AfEno1	25	9	36

Note: The table shows the summary of the CD4$^+$ memory T-cell responses to CaEno1, AfEno1, PPD, Td, and PepTivator *C. albicans* MP65 for all healthy donors tested.
Abbreviation: CaEno1, *C. albicans* Eno1; PPD, purified protein derivative.

(Fig. 3C). Intracellular cytokine staining for IFN-γ secretion, further, showed that 10–25% of cells secreted the cytokine to different degrees (Supporting information Fig. 6C–F) ruling out the possibility that a small contaminating population of memory T cells was the source of cytokine secretion in our assays. CaEno1, thus, skewed naïve CD4$^+$ T-cell responses primarily toward Th2.

Human memory CD4$^+$ T-cell responses are inhibited by CaEno1 in donors with no CD4$^+$ T-cell immunity to CaEno1

To determine whether CaEno1 binding to CD4 interferes with T-cell activation triggered by TCR–peptide/HLA class II interaction, we studied human memory CD4$^+$ T-cell responses to different recall antigens using carboxyfluorescein succinimidyl ester (CFSE) dilution for memory CD4$^+$ T-cell detection (Fig. 4A, Table 1). Among the different recall antigens tested, the response rate of CD4$^+$ T cells from healthy blood donors was highest for the mycobacterial antigen purified protein derivative (PPD), followed by diphtheria and tetanus toxoid (Td), CaEno1, *A. fumigatus* Eno1 (AfEno1), an MP65-derived peptide pool of *C. albicans*, and a pp65-derived peptide pool of CMV (Table 1). Analysis of cytokine concentrations in supernatants of CaEno1-stimulated peripheral blood mononuclear cell (PBMC) revealed strong IFN-γ secretion for most donors (Supporting information Fig. 7). Addition of CaEno1 to PPD or Td reduced recall responses of human CD4$^+$ T cells to PPD and Td (Fig. 4B and Supporting information Fig. 8). To systematically study recall responses of CD4$^+$ T cells from different donors, we focused on PPD as a recall antigen. We observed that recall responses to PPD were unanimously reduced, albeit to different degrees, in the presence of CaEno1 (Fig. 4C). In contrast, CD4$^+$ T cells from donors with immunity against both PPD and/or Td and CaEno1 responded more strongly in the presence of PPD and/or Td and CaEno1 compared to CD4$^+$ T cells cultured in the presence of PPD or Td only (Fig. 4D and Supporting information Fig. 9A–C). To rule out that the contamination of

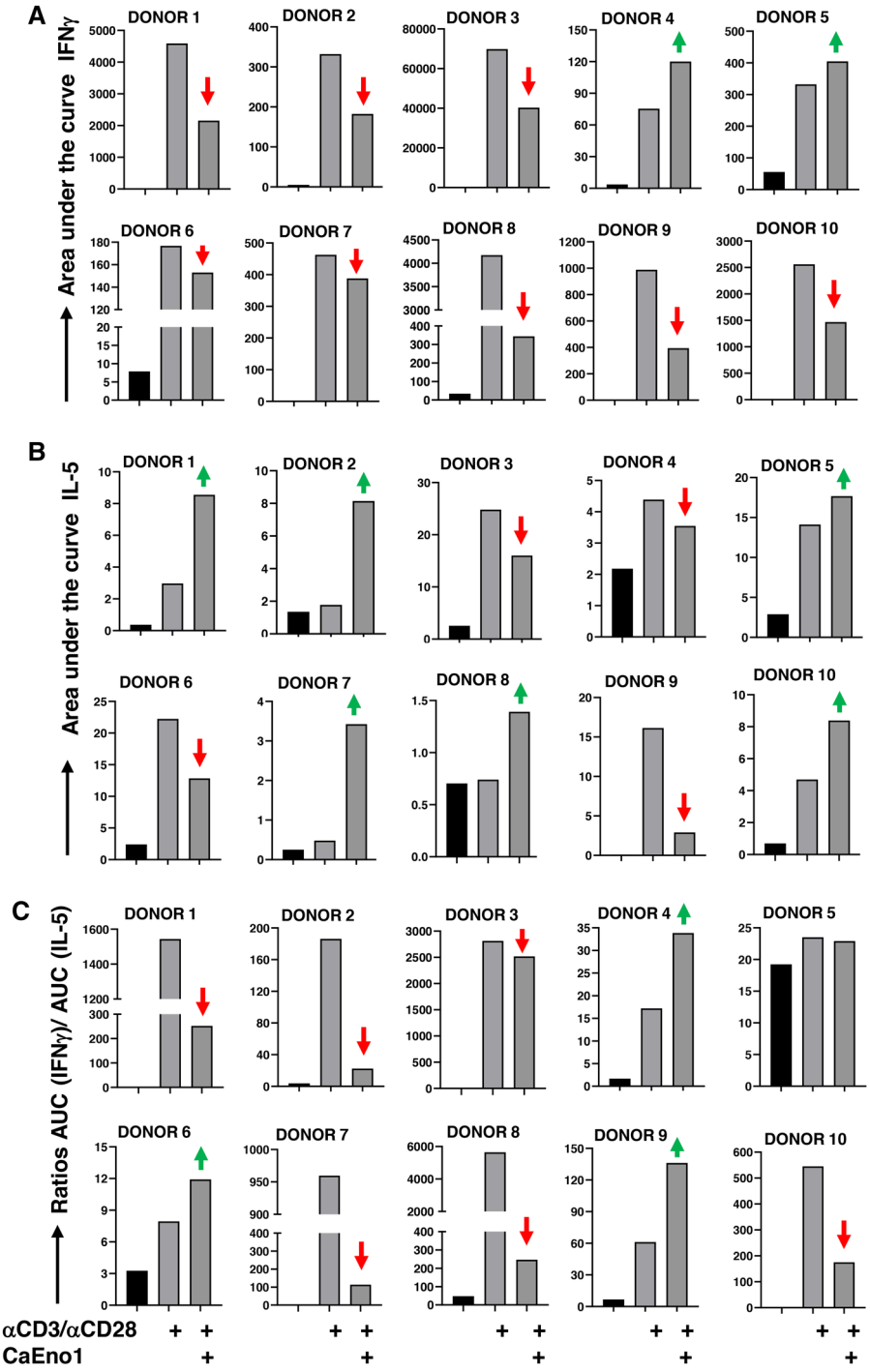

Figure 3. For the majority of healthy blood donors, *Candida albicans* Eno1 (CaEno1) induced Th2-biased responses of naïve CD4$^+$ T cells. Naïve CD4$^+$ T cells were isolated from human peripheral blood mononuclear cells (PBMCs) (n = 10 donors/experiments) and stimulated with Dynabeads Human T-Activator CD3/CD28 in the presence/absence of CaEno1 for up to 3 days. Cytokine content in culture supernatants was determined for each day of culture and the area under the curve (AUC) was calculated for (A) IFN-γ, (B) IL-5, and (C) the ratios of AUC(IFN-γ)/AUC(IL-5). Arrows indicate values differing ≥10% from controls, that is, costimulated naïve CD4$^+$ T cells in the absence of CaEno1.

the CaEno1 preparation with *Escherichia coli*–derived factors like LPS [32] would account for the CaEno1-induced inhibition of PPD responses we also tested CaEno1 expressed and purified from the yeast *Pichia pastoris*. *P. pastoris*–derived CaEno1 was similarly efficient as *E. coli*–derived CaEno1 in suppressing PPD-specific memory CD4$^+$ T cells (Fig. 4E). Apart from CaEno1 also anti-CD4 mAb RPA-T4 and OKT-4 inhibited recall responses of memory CD4$^+$ T cells to PPD (Supporting information Fig. 9D and E). Therefore, CaEno1 constitutes a recall antigen for CD4$^+$ T cells of donors with preexisting immunity and an immunomodulator for CD4$^+$ T-cell recall responses toward unrelated antigens—in our case PPD.

Suppression of CD4$^+$ T-cell recall responses by CaEno1 is independent of functional avidity

The different susceptibility of CD4$^+$ T cells from different donors toward inhibition by CaEno1 could be explained by differences

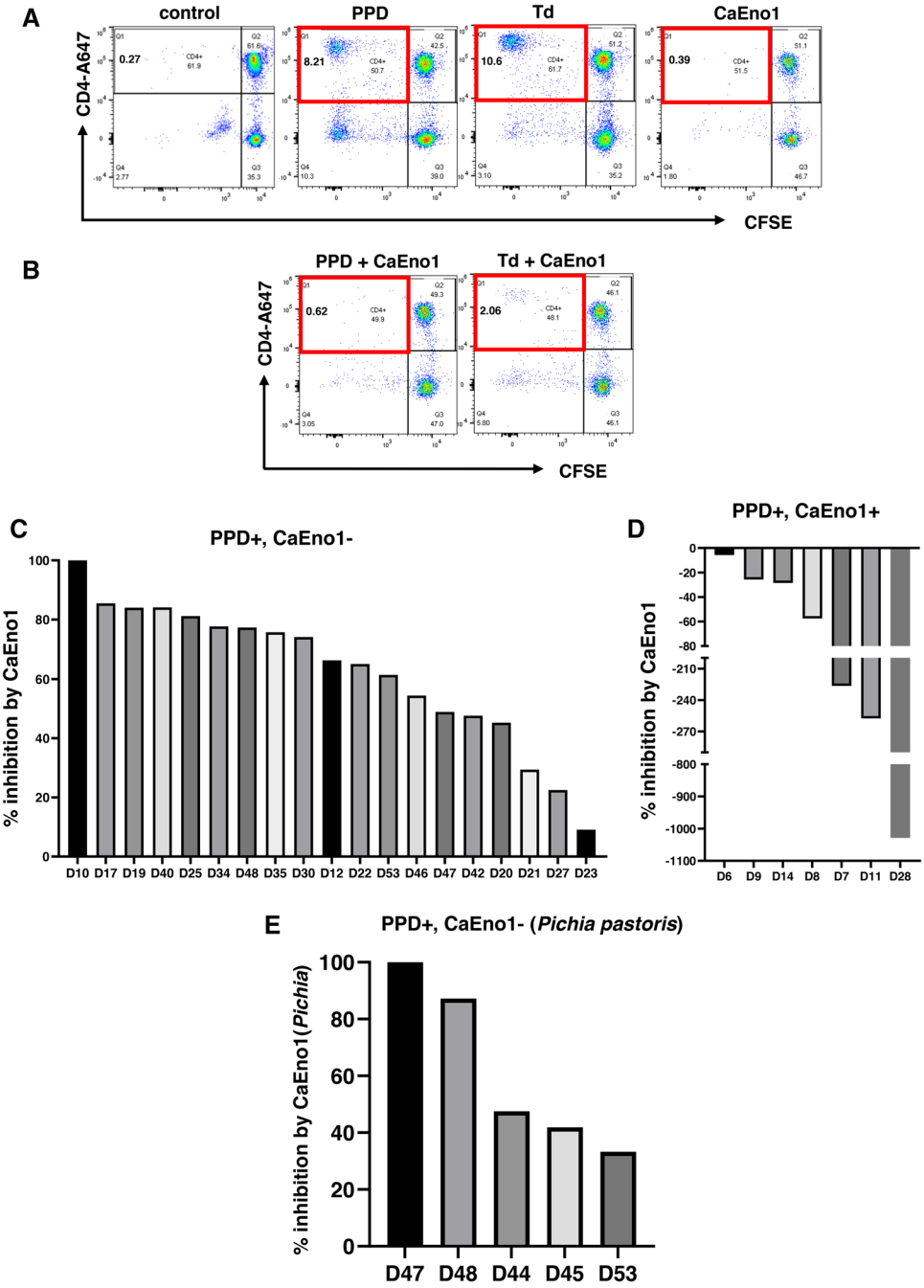

Figure 4. *Candida albicans* Eno1 (CaEno1) inhibited the recall response of memory CD4$^+$ T cells. (A) Human peripheral blood mononuclear cells (PBMCs) (donor: DD10) were stained with carboxyfluorescein succinimidyl ester (CFSE) and cultured in the presence of recall antigens: purified protein derivative (PPD), tetanus and diphtheria toxoid (Td), and CaEno1. Cells cultured in medium only served as negative control (control). On day 6, cells were stained for CD4, and the percentage of CFSE^{low} cells was determined among CD4$^+$ T cells. (B) Parallel cultures of part (A) (PPD and Td) in the presence of CaEno1. (C) % inhibition of recall response to PPD by CaEno1 was calculated taking into account background proliferation (control; complete inhibition of recall response = 100%; $n = 11$ donors/experiments). Results for individual donors without (PPD$^+$ CaEno1$^-$) and (D) with CD4$^+$ T-cell immunity to CaEno1 (PPD$^+$ CaEno1$^+$; $n = 7$ donors/experiments) are shown. (E) % inhibition of recall response to PPD by CaEno1 expressed in *Pichia pastoris* (PPD$^+$ CaEno1$^-$; $n = 5$ donors/experiments).

in the functional avidity of the CD4$^+$ T-cell response to the recall antigen PPD. Therefore, we determined the functional avidity using a limiting dilution assay [33], that is, by serially titrating the concentration of PPD used in the recall assay with CFSE dilution again as the read-out for CD4$^+$ T-cell responses (Fig. 5A and Supporting information Fig. 10). We interpolated the dose–response curve of the PPD titration to determine EC_{50} values as an estimate of the functional avidity of the CD4$^+$ T-cell response toward PPD: The lower the EC_{50} value, the higher the functional avidity and vice versa. Plotting the EC_{50} value of the PPD concentration

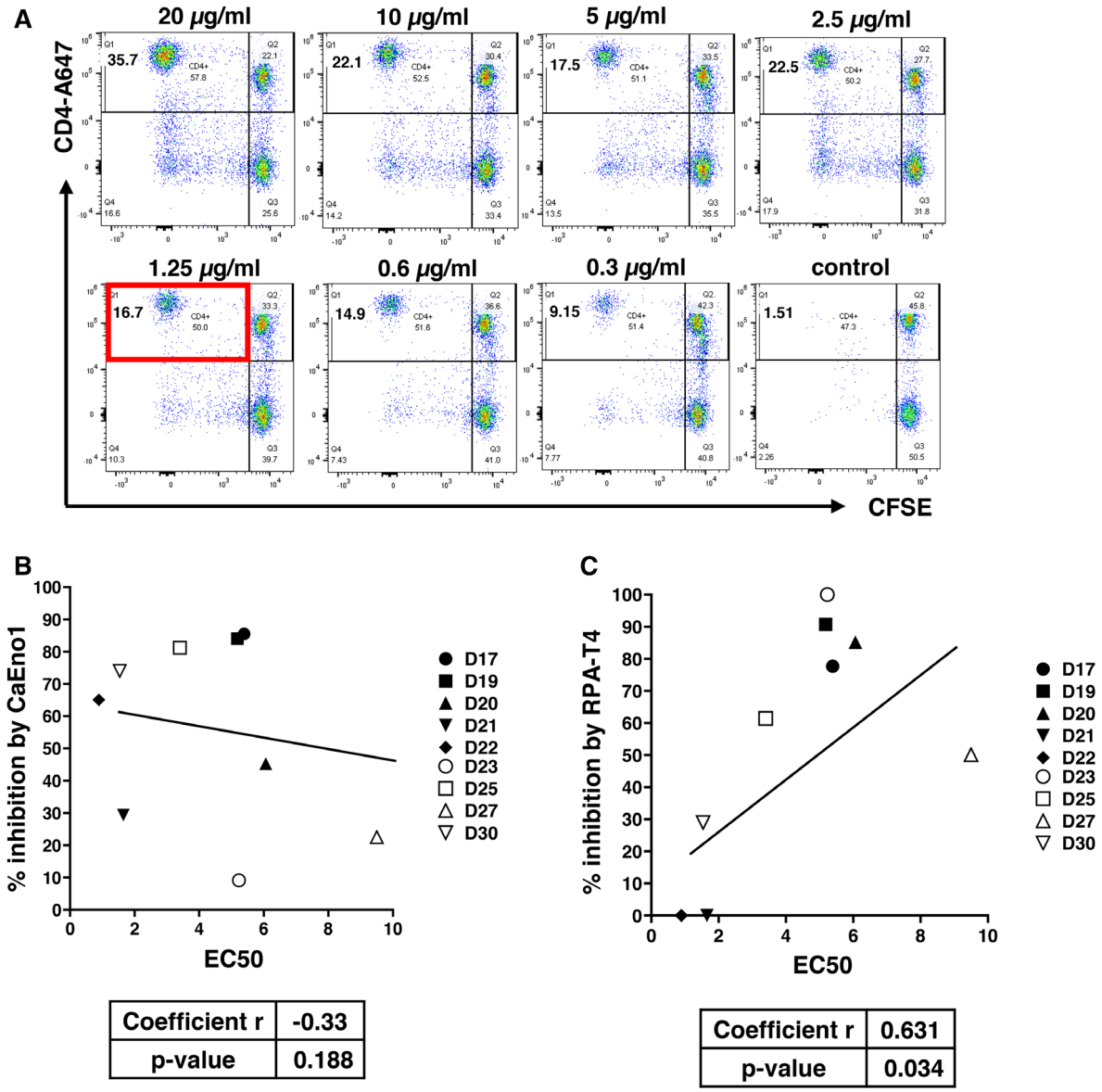

Figure 5. Inhibition of recall responses to purified protein derivative (PPD) by *Candida albicans* Eno1 (CaEno1) was independent of functional avidity. (A) Human peripheral blood mononuclear cells (PBMCs) were stained with carboxyfluorescein succinimidyl ester (CFSE) and cultured for 6 days in the presence of titrated amounts of PPD or without PPD (control) as indicated. From these responses, the EC_{50} value was determined (highlighted in red). One representative data set is shown ($n = 9$ donors/experiments). (B) To determine inhibition, CaEno1 (1 μg/mL) or (C) anti-CD4 monoclonal antibodies (mAb) RPA-T4 (1 μg/mL) were added in addition to PPD (10 μg/mL). The EC_{50} of the PPD response was plotted against the % inhibition of the recall response to PPD by CaEno1 for each donor. Correlations were calculated using GraphPad Prism software.

against the percent inhibition elicited by CaEno1 showed that the degree of inhibition of $CD4^+$ T-cell recalls responses to PPD by CaEno1 did not correlate with the avidity of the T-cell response (Fig. 5B). This was in contrast to the anti-CD4 mAb RPA-T4 for which we observed a negative correlation between the degree of the inhibition of the $CD4^+$ T-cell response by CaEno1 and the functional avidity for PPD (Fig. 5C). Moreover, the frequency of memory T cells responding to PPD also did not determine the susceptibility toward inhibition by CaEno1 (Supporting information Fig. 11). Inhibitions of $CD4^+$ T-cell recall responses to PPD by CaEno1 were, thus, independent of the functional avidity of the T-cell response and the proportion of memory T cells responding.

Human $CD4^+$ T cells transduced with a Crf1 peptide (p41)-specific TCR were not inhibited by CaEno1

Many patients at risk for IFD severely lack innate, but also T-cell immunity due to their underlying disease and/or previous medical interventions [10, 34, 35]. To compensate for this overall lack in immunity, $CD4^+$ T cells with specificity for the

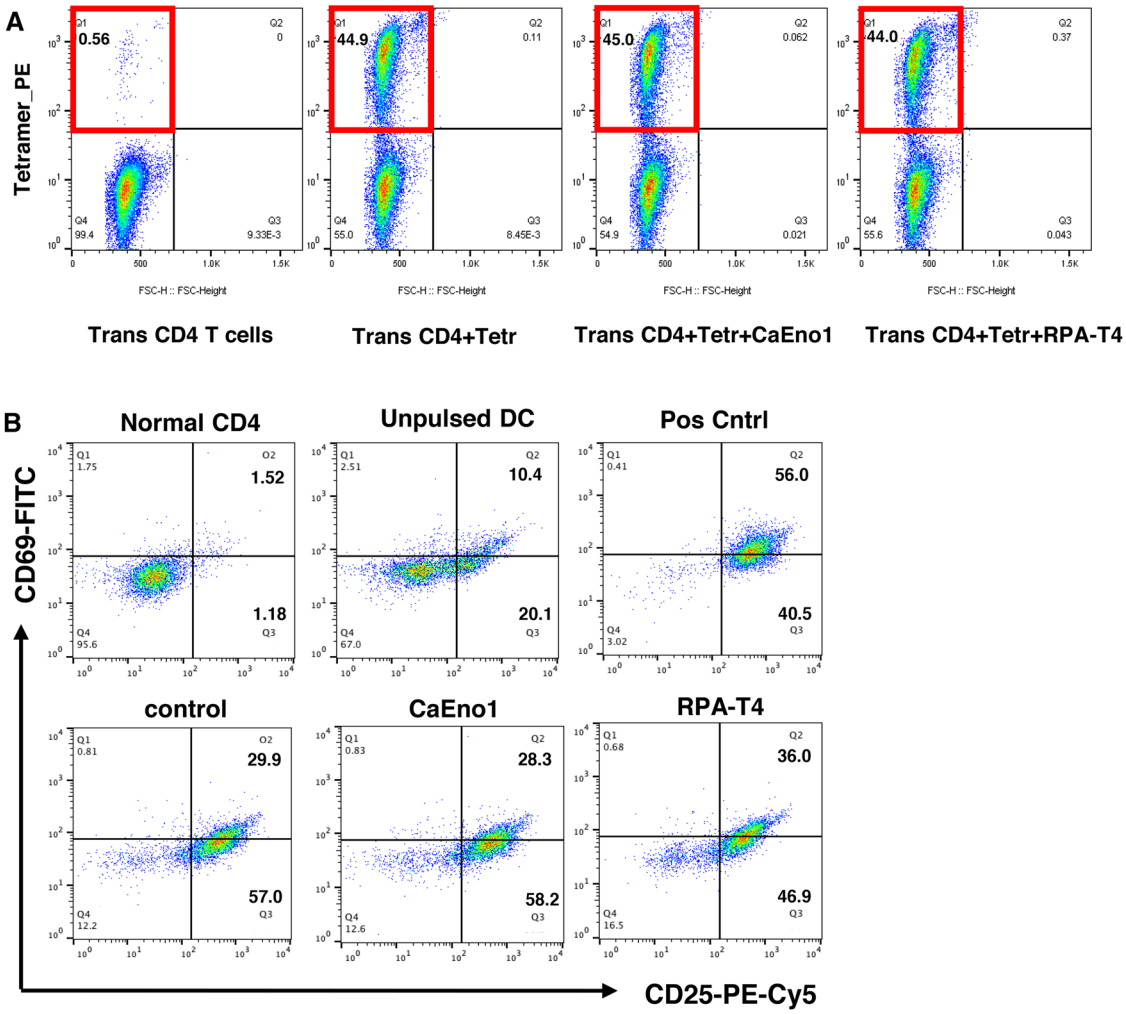

Figure 6. *Candida albicans* Eno1 (CaEno1) neither blocked tetramer binding nor the activation of p41 T-cell receptor (TCR)–transduced CD4$^+$ T cells. (A) p41 TCR–transduced CD4$^+$ T cells were preincubated with CaEno1 or RPA-T4 for 5 min followed by a 30 min incubation with PE-conjugated human leukocyte antigen (HLA)-DRB1*0401 tetramer loaded with Crf1/p41 peptide. Transduced CD4$^+$ T cells without the addition of tetramer (very left dot plot) served as negative control and transduced CD4$^+$ T cells incubated with tetramer only as a positive control (second left dot plot). (B) p41 peptide-pulsed dendritic cells were incubated with p41 TCR–transduced CD4$^+$ T cells in the absence (control) or presence of CaEno1 (1 μg/mL) or RPA-T4 (1 μg/mL) (lower dot plots) for 48 h. Dot plots show the expression of the activation markers CD69 and CD25. Untransduced CD4$^+$ T cells cultured with p41 peptide-pulsed DCs (upper left dot plot) and p41 TCR–transduced CD4$^+$ T cells cultured with unpulsed DCs (upper middle dot plot) were taken as negative controls, whereas p41 TCR–transduced CD4$^+$ T cells cultured with Dynabeads Human T-Activator CD3/CD28 functioned as positive controls (upper right dot plot). (A and B) Representative results from a single experiment of a total of two different experiments with similar results are shown.

p41 peptide of Crf1 have been shown to mediate protection against *C. albicans* and *A. fumigatus* infections [36]. Instead of expanding p41-specific T cells, the transduction of CD4$^+$ T cells with a p41-specific TCR (Supporting information Fig. 12) reduces culturing times in the lab and provides the opportunity to generate off-the-shelf products for T-cell immunotherapy. We, thus, analyzed the impact of CaEno1 on the binding of an HLA-DRB1*0401 tetramer loaded with the p41 peptide to CD4$^+$ T cells transduced with a p41-specific TCR (Fig. 6A). Neither CaEno1 nor the anti-CD4 mAb RPA-T4 blocked tetramer binding to the TCR-transduced CD4$^+$ T cells. Moreover, the activation of the p41 TCR-transduced CD4$^+$ T cells by p41-petide-pulsed HLA-DRB1*0401-expressing dendritic cells was neither inhibited by CaEno1 nor RPA-T4 (Fig. 6B). Therefore, the antigen and activation of p41 TCR-transduced CD4$^+$ T cells were not susceptible to CaEno1-mediated immune evasion.

Discussion

This study found that Eno1 of *C. albicans* binds to human CD4 as predicted bioinformatically. Moreover, CaEno1 binding to CD4 not only had biochemical consequences for the T cells in that LCK was phosphorylated, but CaEno1 also modulated cellular responses of naïve and memory CD4$^+$ T cells.

From the data we have generated so far, we can, however, not say how much LCK phosphorylation by CaEno1 contributes to the modulation of T-cell response. For anti-CD4 mAb, it has been shown that all anti-CD4 mAb, including Tregalizumab, induce LCK activation upon binding albeit to varying degrees [9]. Despite inducing LCK phosphorylation, Tregalizumab is thought to mediate antiinflammatory effects in vivo through the activation of $CD4^+$ $Foxp3^+$ regulatory T cells (reviewed in Ref. [37]). Therefore, for anti-CD4 mAb, there is a complex relationship between the phosphorylation-inducing activity on the receptor and the capacity of such antibodies to mediate immunomodulation. For CaEno1 and CD4, the situation appears to be similarly complex.

Mapping of CaEno1 binding to CD4 revealed that domain 3 was critically involved in the CaEno1–CD4 interaction (Fig. 1). This is in contrast to gp120 of the HIV, which binds domain 1 of human CD4, thus initiating the infection of $CD4^+$ T cells [38]. We observed that CaEno1, indeed, did not inhibit the infection of CD4-expressing cell line cells with HIV-1 (Supporting information Fig. 4). This observation in turn means that the increased risk of HIV infection, which is associated with genital candidiasis [39], may in part be due to CaEno1 not inhibiting infection of $CD4^+$ T cells with the virus. The therapeutic anti-CD4 mAb Tregalizumab binds domain 2 of CD4 and induces activation of $CD4^+$ $Foxp3^+$ regulatory T cells (reviewed in Ref. [37]). Currently, we do not know whether CaEno1 also has an effect on $CD4^+$ $Foxp3^+$ regulatory T cells despite binding to a different domain of CD4. As detailed below, we focused our functional characterization on the consequences of CaEno1 binding to naïve and memory conventional, that is, nonregulatory, $CD4^+$ T cells.

When we costimulated naïve $CD4^+$ T cells with Dynabeads T-Activator CD3/CD28, we observed that IFN-γ secretion was reduced in eight out of ten experiments with cells from healthy blood donors (Fig. 3). IFN-γ secretion by human naïve $CD4^+$ T cells activated for 3 days with Dynabeads Human T-Activator CD3/CD28 has been described with very similar frequencies to the ones reported by us [40]. The early glycolytic switch of activated naïve $CD4^+$ T cells [40] favors IFN-γ expression by preventing GAPDH from binding to IFN-γ mRNA [41]. In five of the eight experiments, lower IFN-γ secretion was accompanied by higher IL-5 secretion. Therefore, CaEno1 might actively contribute to the skewing of anti–*C. albicans* Th–cell responses in vivo toward Th2 and thereby mediates immune evasion [10]. Currently, it is unclear what role the interaction of CaEno1 with CD4 plays in the modulation of naïve $CD4^+$ T-cell responses as we have shown that CaEno1 also binds to leukocytes, which do not express CD4—most prominently B cells [42]. This means that CaEno1 can be expected to interact with additional molecules on the surface of $CD4^+$ T cells, and these interactions might contribute to the modulation of naïve $CD4^+$ T-cell responses by CaEno1.

Upon antigen recognition, CD4 plays a key role in stabilizing TCR–peptide/HLA interactions and, of course, recruits LCK to the immunological synapse (reviewed in Refs. [7, 8]). We, thus, studied the impact of CaEno1 on antigen-driven recall responses by human memory $CD4^+$ T cells. Here, we first noted that in about 40% of donors, CaEno1 served as a potent stimulus for CaEno1-specific $CD4^+$ T cells (Table 1). Although ($CD4^+$) T-cell responses to Eno1 of *A. fumigatus* have been studied in humans [21, 24], our study is, to the best of our knowledge, the first to provide information on CaEno1-directed $CD4^+$ T-cell immunity. Strong IFN-γ secretion by CaEno1-stimulated PBMC (Supporting information Fig. 7) indicates that the CaEno1-specific memory $CD4^+$ T-cell response induced in healthy subjects is suitable to provide protection against *C. albicans*. The lack of a memory $CD4^+$ T-cell response in about 60% of healthy blood donors, in turn, corroborates the notion that in many patients with IFD naïve $CD4^+$ T cells will be recruited to mediate protection against the disease.

Among all recall antigens tested, we observed the highest response rate for PPD to which memory $CD4^+$ T cells of 68% of human blood donors responded in our study (Table 1). PPD-specific recall responses were, however, inhibited by CaEno1 to varying degrees when there were no CaEno1-specific memory cells in the $CD4^+$ T-cell compartment (Fig. 4). We, thus, observed that CaEno1 interferes with physiological antigen recognition by T cells. Variability in domain 3 of CD4 leading to stronger or weaker interaction with CaEno1 might be a reason for the range of responses observed for different donors. Substitution of tryptophan for arginine at position 240, that is, within domain 3 of the extracellular domain of CD4, has been reported for some individuals leading to a loss of the epitope for anti-CD4 mAb OKT-4 [43–45]. Similar to allogeneic mixed lymphocyte reactions [46], the anti-CD4 mAb RPA-T4 also inhibited memory $CD4^+$ T-cell responses to PPD (Fig. 5). In contrast to CaEno1, the degree of inhibition mediated by RPA-T4 negatively correlated with the functional avidity of the memory $CD4^+$ T-cell response, which we assume is due to the binding of RPA-T4 to domain 1 of CD4, thus interfering with CD4–peptide/HLA interactions. Our assay system was, thus, not only suitable to determine functional avidity but also to pick up correlations between the degree of inhibition of $CD4^+$ T-cell responses by a reagent and functional avidity.

A side-by-side comparison of RPA-T4 and OKT-4 showed that also the binding of OKT-4 to domain 3 of CD4 inhibited T-cell responses to PPD (Supporting information Fig. 9D and E). This highlights that targeting of domain 3 is suitable/sufficient to inhibit the activation of memory $CD4^+$ T cells by antigen, which to the best of our knowledge we are the first to report.

During a primary immune response, it is low-affinity $CD4^+$ T cells that primarily respond to antigen [33]. Increases in the functional avidity of the $CD4^+$ T-cell response upon prolonged antigen exposure/the memory phase of an immune response then allow for the efficient clearance of, for example, SARS-CoV-2, whereas the "overstimulation" of low-affinity $CD4^+$ T cells is thought to mediate immunopathology [47].

Patients at risk of developing or already suffering from IFD caused by *C. albicans* or *A. fumigatus* often have severely impaired innate, but also T-cell immunity, including a lack of cells with specificity for fungal antigens. Adoptive transfer of antifungal T cells, thus, constitutes an efficacious way of restoring antifungal immunity. With the p41 peptide of Crf1, there is an antigen specificity that allows generating T cells to mediate protection against both *C. albicans* and *A. fumigatus* [36]. Of course, such T cells can

Table 2. Relationship of $CD4^+$ memory T-cell responsiveness to *Candida albicans* Eno1 (CaEno1) versus AfEno1.

		25		Total
Response to AfEno1	+	2	6	25
	−	13	4	
		−	+	
		Response to CaEno1		

Note: The table shows the summary of the responses to CaEno1 and AfEno1. Fisher's exact test: $p = 0.03$.

also become the target of fungal immune evasion mechanisms that, in a worst case scenario, would even be strong enough to overcome the protection mediated by the adoptively transferred T cells. p41 TCR-transduced $CD4^+$ T cells, however, appeared to be exempt from inhibition by CaEno1 (Fig. 6). As the functional avidity and suppression of memory $CD4^+$ T-cell responses by CaEno1 did not correlate (Fig. 5), it is currently unclear which factors determine susceptibility to suppression by CaEno1 and how to avoid these when designing strategies to prevent and/or treat IFD with T-cell products. However, with the p41 TCR, a candidate is available, which can be expected to provide immunity against *C. albicans* and *A. fumigatus* in vivo despite the secretion of Eno1 by the fungi.

Eno1 of *A. fumigatus* (AfEno1) has 73% identity with CaEno1 at the amino acid level, and at least in some donors, there might be cross-reactive $CD4^+$ T cells against both enolases (Table 2). Similar to CaEno1, AfEno1 also is a moonlighting protein mediating immune evasion [19]. In addition, we noted that AfEno1 was also capable of binding to CD4 (Supporting information Fig. 2) as predicted [1, 2].

Apart from pathogens, of course, also the human host expresses (human) Eno1 (hEno1). Expression at the cell surface and secretion of hEno1 by cancer cells [48] means that hEno1 might also mediate immune evasion through binding to CD4. Testing recombinantly expressed hEno1 in the FACS-based binding assay, which we also used to study the interaction of CaEno1 with CD4 (Fig. 1), however, revealed that hEno1 did not bind CD4 (Supporting information Fig. 3). Interference with $CD4^+$ T-cell activation through the secretion of hEno1, thus, does not appear to constitute a cancer immune evasion mechanism.

In summary, our study provides evidence that the interaction of CaEno1 with CD4 on $CD4^+$ T cells, which was predicted by bioinformatical means, indeed might occur during fungal infections with *C. albicans*. Our data, further, suggest that this interaction is capable of modulating both naïve and memory $CD4^+$ T-cell responses. In hosts with no preexisting immunity against CaEno1, our results imply that this will very likely lead to a Th2 skewing of newly recruited ("naïve") $CD4^+$ T cells and to an inhibition of potentially cross-reactive preexisting memory T cells. Taken together, this constitutes a substantial degree of immune evasion, which might have detrimental consequences for the patient. This argues in favor of developing methods/vaccines for inducing CaEno1-specific memory T cells in patients at the risk of developing an IFD. Alternatively, p41 TCR–transduced T cells might be used to restore antifungal immunity by providing the right TCR specificity and by avoiding CaEno1-mediated immune evasion.

Methods

Coating of recombinant human CD4 on Dynabeads M-270 Epoxy beads

Dynabeads M-270 Epoxy of 2×10^7 were washed three times with 0.1 M Na phosphate buffer pH 8 (200 μL). In each washing step, beads were pelleted for 4 min on a magnet. Na phosphate buffer pH 8 of 0.1 M (70 μL), ammonium sulfate pH 7.4 of 3 M (70 μL), and recombinant human CD4 of 10 μg (Thermo Fisher Scientific) in PBS (70 μL) were added to the washed beads and kept on a rotator in a cold room (4°C) for 72 h. Beads were vortexed daily. On day 3, beads were washed four times with PBS/0.1% BSA. Finally, the CD4-coated beads were stored in sterile PBS/0.1% BSA/0.02% NaN_3 (200 μL) at 4°C. The beads were analyzed for CD4 coating by flow cytometry using the FACS Diva software (all Becton Dickinson, Franklin Lakes, NJ, USA). Data were analyzed with FlowJo software [9.9.6/10.5.3] (TreeStar Inc., Ashland, OR, USA).

Expression and purification of CaEno1

CaEno1 was expressed in *E. coli* and purified as previously described for Eno1 from *A. fumigatus* [19]. Alternatively, we expressed CaEno1 in *P. pastoris*. For this, the CaENO1 gene was PCR-amplified from the genomic DNA of *C. albicans* strain Sc5314SC5314 using the forward primer Eno1_C_F (5′-tccgcgGGTACCctATGTCTTACGCCACTAAAATCC-3′) and the reverse primer Eno1_C_R (5′-gcgcctTCTAGAtcCAATTGAGAAGCCTTTTGGAAA-3′), harboring the restriction sites (underlined) of Kpn IKpnI and Xba IXbaI. The target amplicon and pPICZαB vector (Invitrogen) were digested with Kpn IKpnI and Xba IXbaI and ligated via T4 DNA ligase (New England Biolabs), followed by subsequent transformation into *E. coli* Top10 (Invitrogen). The plasmid harboring CaENO1 gene (pPICZαB-CaENO1) was purified from *E. coli* Top10 and further used for subcloning into *P. pastoris* X33 (Invitrogen). The CaEno1 was expressed in *Pichia* as a His-tagged protein. After 4 days of the induction of expression using 1% methanol, the protein was harvested and purified from the culture supernatant using Ni-NTA Agarose (Qiagen) according to the manufacturer's protocol.

CaEno1 binding assay

Human CD4-coated beads (2×10^4) were incubated with CaEno1 (1 μg/mL) in PBS/0.1% BSA/0.02% NaN_3. A rabbit antiserum

against CaEno1 (1:1000) as primary and donkey-anti-rabbit IgG (H + L) antibody (Jackson ImmunoResearch) (1:200) as secondary antibody were used to detect CaEno1 bound to human CD4 immobilized on epoxy beads. After every incubation step (20 min, 4°C), beads were transferred to a new well and washed twice with PBS.

Epitope mapping of CaEno1 binding to CD4

Anti-CD4 mAb RPA-T4 (BD Biosciences), tregalizumab (T-Balance), or OKT-4 (BioLegend), which bind domains 1–3 of human CD4, respectively, were used to compete with the binding of CaEno1 (1 μg/mL) to human CD4 coated on Dynabeads M-270 Epoxy. CD4-coated beads (2×10^4) were incubated with RPA-T4 (1 μg/mL) or Tregalizumab (1 μg/mL) or OKT-4 (1 μg/mL) (20 min, 4°C). CaEno1 (1 μg/mL) was added to the beads and incubated for 20 min at 4°C. Beads were transferred to a new well, to avoid binding of the secondary antibody to the well surface, and washed twice with PBS. CaEno1 binding was detected by rabbit-anti-CaEno1 (1:1000) and an A647-conjugated donkey-anti-rabbit IgG (H + L) as secondary antibody (Jackson ImmunoResearch) (1:200).

Preparation of human peripheral blood mononuclear cells (PBMCs)

Human PBMCs were isolated from the blood of healthy donors. Briefly, concentrated blood samples were diluted 1:1 with PBS. PBMCs were then isolated by density gradient centrifugation with Histopaque-1077 (Sigma) and washed with BSS/0.1% BSA twice. Finally, PBMCs were resuspended in RPMI 1640 Medium containing L-Glutamine (Gibco) and supplemented with 1% Sodium pyruvate 100 mM (100×) (Gibco), 1% HEPES buffer solution 1 M (Gibco), 100 U/mL penicillin/100 μg/mL Streptomycin (Sigma), 0.1% 2-Mercaptoethanol 50 mM (Gibco), 1% MEM NEAA (100×) (Gibco), and 10% human AB serum (Sigma) ($RPMI^+$ medium). Cells were diluted with Trypan blue and counted in a Neubauer counting chamber to determine the number of viable cells.

$CD4^+$ T-cell enrichment

$CD4^+$ T cells were isolated from PBMCs by magnetic depletion (negative selection) according to the manufacturer's instructions (Miltenyi Biotec). In brief, PBMCs were mixed with a cocktail of biotin-conjugated mAb (CD8α, CD14, CD15, CD16, CD19, CD36, CD56, CD123, TcRγ/δ, and CD235a (glycophorin A)) recognizing all cells except for $CD4^+$ T cells followed by antibiotin microbeads. The mixture was finally passed through an LS column (max. 10^8 cells/LS column) placed in the magnetic field of a MACS separator. The flow-through contained unlabeled and untouched enriched $CD4^+$ T cells. The purity of $CD4^+$ T cells was analyzed by flow cytometry (average purity ± SD: 91% ± 3).

Quantification of LCK phosphorylation

Purified $CD4^+$ T cells (1×10^5) were incubated with CaEno1 (1 μg/mL), H_2O_2 (5 mM), anti-CD4 mAb RPA-T4 (BD Biosciences, 1 μg/mL), or anti-CD3ε mAb HIT3a (BioLegend, 1 μg/mL) in pre-warmed $RPMI^+$ medium in a 96-well round-bottom plate (30 min, 37°C). After the incubation, cells were transferred to a 96-well V-bottom plate, fixed with 2% paraformaldehyde (20 min, room temperature), washed with PBS, and then, permeabilized with 96% methanol (−20°C overnight). The next day, cells were split into two wells, and intracellular staining was performed with an anti-phospho-LCK(Tyr505) (clone A17013A) or an anti-phospho-LCK(Tyr394) (clone A18002D) mAb (45 min, room temperature, in the dark).

The cells were analyzed on a BD LSR II flow cytometer (Becton Dickinson, Franklin Lakes, NJ, USA) or an Attune NxT Flow Cytometer (Thermo Fisher Scientific, Dreieich, Germany). For further analyses of the data, FlowJo (TreeStar Inc., Ashland, OR, USA) software was used.

Naïve $CD4^+$ T-cell isolation

Naïve $CD4^+$ T cells were isolated from PBMCs by magnetic depletion (negative selection) according to the manufacturer's instructions (Miltenyi Biotec; anti-CD8, CD14, CD15, CD16, CD19, CD25, CD34, CD36, CD45RO, CD56, CD123, TCRγ/δ, HLA-DR, and CD235a (Glycophorin A)). The purity of naïve $CD4^+$ T cells was analyzed by flow cytometry (average purity ± SD: 93% ± 3).

Naïve $CD4^+$ T-cell culture

Naïve $CD4^+$ T cells were cultured in $RPMI^+$ medium (2×10^5 cells/well, 96-well U-bottom plate) with Dynabeads Human T-Activator CD3/CD28 (1 bead/cell) (Thermo Fisher Scientific), in the presence or absence of CaEno1 (1 μg/mL). Cells cultured in $RPMI^+$ medium only served as unstimulated negative control in the study. The culture plates were kept in the incubator at 37°C for 3 days. Each day, about 100 μL of culture supernatant were removed to determine the concentration of the cytokines secreted by the cells.

Human cytokine analysis in culture supernatants

The concentrations of IFN-γ, IL-2, IL-4, IL-5, IL-6, IL-10, IL-13, IL-17A, IL-22, and TNF-α were analyzed in the culture supernatant using the LEGENDplex bead-based immunoassay (BioLegend) according to the manufacturer's instructions.

Detection of cytokine secretion by intracellular staining

Cells were restimulated with 5 ng/mL phorbol 12-myristate 13-acetate (PMA) and 500 ng/mL Ionomycin (all Sigma) at 37°C and in the presence of 5% CO_2 for 2 h. To prevent cytokine secretion, cells were incubated with 10 μg/mL brefeldin A (Sigma) for a further 2 h. Cells were transferred to a 96-well V-bottom plate, and surface staining was performed as described above. Afterward, cells were washed with PBS and fixed with Fixation buffer (Fix/Perm buffer, eBioscience) (30 min, 4°C). An antibody mix for intracellular staining containing anti-IFN-γ-PE-Cy7 and anti-IL-5-PE in perm buffer was added, and cells were kept in the dark (45 min, room temperature). Cells were washed with perm buffer followed by another washing step with FACS buffer. Finally, the cells were resuspended in FACS buffer and analyzed on an LSR II (Becton Dickinson). Data were further analyzed with FlowJo software (TreeStar).

Antigenic recall responses

After two washes with protein-free buffer, PBMCs were labeled with CFSE diacetate (Thermo Fisher Scientific, 5 μM, 1×10^7 cells/mL, 5 min, room temperature) followed by addition and two washes with buffer containing 0.1% BSA. Cells (2×10^5 cells/well) were cultured in a U-bottom plate with 10 μg/mL PPD (Pharmore), 100 mU/mL tetanus and diphtheria toxoid (Td)-RIX (GlaxoSmithKline), 0.6 nM PepTivator *C. albicans* MP65 (Miltenyi Biotec), or 0.6 nM PepTivator CMV pp65 (Miltenyi Biotec) in the presence or absence of 1 μg/mL CaEno1 for 6 days at 37°C. Recall responses to 1 μg/mL AfEno1 [19] were also analyzed.

Determination of functional avidity

CFSE-labeled PBMCs of 2×10^5 were cultured in RPMI$^+$ medium for 6 days at 37°C with titrated amounts of PPD (Pharmore), that is, 10, 5, 2.5, 1.25, 0.6, 0.3, and 0 μg/mL, in the presence or absence of 1 μg/mL CaEno1 or 1 μg/mL anti-CD4 mAb (RPA-T4).

FACS analysis of antigenic recall responses

To determine the proliferation of CFSE-labeled CD4$^+$ T cells, the cultured PBMCs were first incubated with 0.2 μg/mL anti-CD4 mAb RPA-T4 in PBS/0.1% BSA/0.02% NaN_3 (15 min, 4°C). Cells were washed twice, transferred to a new well, and washed again with PBS/0.1% BSA/0.02% NaN_3 followed by incubation with goat anti-mouse IgG + IgM (Jackson ImmunoResearch 0.5 μg/mL) (15 min, 4°C). Cells were washed twice with PBS. Finally, cells were stained with Viability Dye after a blocking step with normal mouse Ig. Samples were measured and analyzed on an Attune NxT Flow Cytometer (Thermo Fisher Scientific), and data were analyzed with FlowJo software.

p41 peptide-specific TCR cloning and transduction of CD4$^+$ T cells

The Crf1/p41-peptide (FHTYTIDWTKDAVTW) was obtained from ProImmune. A T-cell clone specific for this peptide was isolated as described before [49].

mRNA encoding the p41-specific TCR was then isolated from the p41-specific T-cell clone using the RNeasy Mini Kit (Qiagen), and cDNA was synthesized by SMARTer RACE cDNA amplification (Clontech Laboratories) as recommended by the manufacturer. Briefly, cDNA was synthesized by SMARTer RACE rtPCR generating amplicons with additional oligonucleotides at the 5′ end (Supporting information Fig. 12). The synthesized cDNA was used for the PCR reaction with the SMARTer RACE universal primer mix and the PACE a rev (GGTGAATAGGCAGACAGACTT) or RACE b rev primer (GTGGCCAGGCACACCAGTGT). The next PCR reaction was performed with a Universal primer A Mix and a reverse primer that binds to the constant region of the alpha (TCRaC rev EcoR1 AGCTTGGAATTCTCAGCTGGACCACAGCCGCAGC) or the beta chain (TCRbC1 rev EcoR1 AGCTTGGAATTCTCAGAAATC-CTTTCTCTTGACC or TCRbC2 rev EcoR1 AGCTTGGAATTC-CTAGCCTCTGGAATCCTTTCTC). The PCR product was then sequenced by GATC-Biotech (Konstanz), and sequences were analyzed by comparing to the database sequences from Immunogenetics (IMGT) (Lefranc 2004). Once the variable regions were identified, the full-length TCR-coding sequence was designed and the cloning into the pMP71 vector was performed by GeneArt (Regensburg, Germany). The sequence was codon optimized. The alpha and beta chains were cloned as a single open reading frame separated by a P2A linker. To avoid mispairing, constant regions were replaced by murine constant regions, and an additional disulfide bond was introduced between them.

To obtain higher amounts of plasmid, DH5alpha competent T cells (Invitrogen) were transformed, and the pMP71-p41 TCR was isolated by Mini- (Qiagen) and Maxiprep (Machery and Nagel), quantified by Multiskan (Thermo Scientific) and qualified via an EcoR I, Not I (NEB) digestion. Retrovirus containing the p41 TCR was produced as a supernatant of the Platinum A cell line (Cell Biolabs). Briefly, PlatA cells were cultured overnight with 4×10^5 cells in 1.6 mL DMEM (Lonza)/10% FCS (Merck), transfected with 3 μg p41 TCR vector DNA and 2 μg pCMV-VSV-G envelope vector DNA and Effectene Transfection Reagent (Qiagen), incubated overnight at 37°C and after medium change 24–48 h at 32°C for virus production. Supernatant was harvested, concentrated for 1.5 h at 16,100 × *g*, and used for the transduction of ex vivo T cells.

Human CD4$^+$ T cells enriched by a negative selection kit (Miltenyi Biotec) were seeded in a 24-well plate at a concentration of 1×10^6/well in cell culture medium supplemented with 100 U/mL recombinant human IL-2 (rhIL-2, Proleukin, Novartis), activated with Dynabeads T-Activator CD3/CD28 (Thermo Fisher Scientific) and incubated at 37°C/ 5% CO_2. After 48 h, the cells were harvested and separated from the Dynabeads T-Activator CD3/CD28 by magnetic pelleting. The CD4$^+$ T cells (1.6×10^6 cells in 500 μL medium) were transferred to

RetroNectin (Takara)-coated plates (48-well plate) preincubated for 30 min at 32°C with virus-containing concentrated supernatant (500 μL/well). To facilitate infection, the plate containing $CD4^+$ T cells and virus was then centrifuged for 1.5 h at 800 × *g* and 32°C.

p41/Crf1 tetramer staining

p41 TCR-transduced human $CD4^+$ T cells (2×10^4) were seeded into a 96-well U-bottom plate. CaEno1 (1 μg/mL) or anti-CD4 mAb RPA-T4 (1 μg/mL) were added to the cells and incubated for 5 min at room temperature. Cells were then incubated with PE-conjugated-HLA-DRB1*0401 tetramer loaded with the p41 peptide (FHTYTIDWTKDAVTW, MBL) for 30 min at room temperature. Cells were washed with FACS buffer and measured on a BD LSR II flow cytometer.

Antigenic stimulation of p41 TCR transductants

p41 TCR–transduced $CD4^+$ T cells (5×10^4) were incubated with p41 peptide-pulsed (1 μg/mL; 1 h, 37°C, 5% CO_2) human monocyte–derived dendritic cells from an HLA-DRB1*0401-positive donor in the absence or presence of CaEno1 (1 μg/mL) or RPA-T4 (1 μg/mL) at 37°C/5% CO_2. Untransduced $CD4^+$ T cells and p41 TCR–transduced $CD4^+$ T cells co-cultured with unpulsed DCs were used as negative controls, whereas p41 TCR–transduced $CD4^+$ T cells stimulated with Dynabeads Human T-Activator CD3/CD28 (Thermo Fisher Scientific) were used as positive controls in the study. After 24 h, the cells were stained for CD4 (RPA-T4, BD), CD25 (BC96, BioLegend), and CD69 (FN50, Immuno Tools) expression and analyzed by flow cytometry.

Statistical analysis

The area under the curve to integrate cytokine secretion of naïve $CD4^+$ T cells over time was calculated using GraphPad Prism Software. Data were presented as means + SD. A paired *t*-test or the Wilcoxon signed-rank test, the nonparametric equivalent of the paired *t*-test, were performed to determine significant differences using GraphPad Prism Software version 9. *p*-values <0.05 were considered to be statistically significant.

Acknowledgments: We thank Michael Hudecek for providing the expression vector pMP71.
Open access funding enabled and organized by Projekt DEAL.

Conflict of interest: The authors declare no financial or commercial conflict of interest.

Author Contributions: Muhammad Daud performed experiments, analyzed data, and wrote the manuscript. Prasad Dasari performed experiments, analyzed data, and provided reagents. Marion Adelfinger performed experiments, analyzed data, and edited the manuscript. Daniela Langenhorst and Anton Althammer analyzed data and edited the manuscript. Jasmin Lother, Dragana Slavkovic-Lukic, Carsten Berges, Niklas Pallmann, Michaela Kruhm, and Karl Alberter performed experiments and analyzed data. Annette Galler provided reagents and analyzed data. Cathrin Schleussner and Haroon Shaikh provided reagents and edited the manuscript. Christian H. Luther, Andreas Beilhack, and Marcus Dittrich edited the manuscript. Jochen Bodem designed experiments and analyzed data. Mohammed El-Mowafy provided crucial reagents and edited the manuscript. Max S. Topp designed research and analyzed data. Peter F. Zipfel designed research, analyzed data, and edited the manuscript. Niklas Beyersdorf designed research, analyzed data, and wrote the manuscript.

Funding Information: DFG, grants SFB-TR 124 FungiNet, 210879364, projects A3, A4, B2, C6; DAAD; FACS Core Unit of the IZKF Würzburg (Z-12).

Ethics statement: Blood samples were provided by the Department of Transfusion Medicine of the University Hospital Würzburg anonymously as a byproduct of platelet concentrates obtained with leukoreduction system chambers (LRS-C; Gambro Trima Accel aphaeresis apparatus, Pall Corp.) and in accordance with the guidelines of the Ethics Committee of the Medical Faculty of the University of Würzburg.

Data availability statement: The data that support the findings of this study are available from the corresponding author upon reasonable request.

References

1 **Remmele, C. W., Luther, C. H., Balkenhol, J., Dandekar, T., Muller, T. and Dittrich, M. T.**, Integrated inference and evaluation of host-fungi interaction networks. *Front. Microbiol.* 2015. **6**: 764.

2 FungiWeb. https://fungiweb.bioapps.biozentrum.uni-wuerzburg.de

3 **Filion, L. G., Izaguirre, C. A., Garber, G. E., Huebsh, L. and Aye, M. T.**, Detection of surface and cytoplasmic CD4 on blood monocytes from normal and HIV-1 infected individuals. *J. Immunol. Methods* 1990. **135**: 59–69.

4 **Cruikshank, W. and Center, D. M.**, Modulation of lymphocyte migration by human lymphokines. II. Purification of a lymphotactic factor (LCF). *J. Immunol.* 1982. **128**: 2569–2574.

5 **Center, D. M. and Cruikshank, W.**, Modulation of lymphocyte migration by human lymphokines. I. Identification and characterization of chemoattractant activity for lymphocytes from mitogen-stimulated mononuclear cells. *J. Immunol.* 1982. **128**: 2563–2568.

6 **Mathy, N. L., Scheuer, W., Lanzendorfer, M., Honold, K., Ambrosius, D., Norley, S. and Kurth, R.**, Interleukin-16 stimulates the expression and production of pro-inflammatory cytokines by human monocytes. *Immunology* 2000. **100**: 63–69.

7 **Ravichandran, K. S., Collins, T. L. and Burakoff, S. J.**, CD4 and signal transduction. *Curr. Top. Microbiol. Immunol.* 1996. **205**: 47–62.

8 **Rossy, J., Williamson, D. J. and Gaus, K.**, How does the kinase Lck phosphorylate the T cell receptor? Spatial organization as a regulatory mechanism. *Front. Immunol.* 2012. **3**: 167.

9 **Helling, B., Konig, M., Dalken, B., Engling, A., Kromer, W., Heim, K., Wallmeier, H. et al.**, A specific CD4 epitope bound by tregalizumab mediates activation of regulatory T cells by a unique signaling pathway. *Immunol. Cell Biol.* 2015. **93**: 396–405.

10 **Romani, L.**, Immunity to fungal infections. *Nat. Rev. Immunol.* 2011. **11**: 275–288.

11 **Bacher, P., Hohnstein, T., Beerbaum, E., Rocker, M., Blango, M. G., Kaufmann, S., Rohmel, J. et al.**, Human anti-fungal Th17 immunity and pathology rely on cross-reactivity against *Candida albicans*. *Cell* 2019. **176**: 1340–1355.e15.

12 **Netea, M. G., Joosten, L. A., van der Meer, J. W., Kullberg, B. J. and van de Veerdonk, F. L.**, Immune defence against Candida fungal infections. *Nat. Rev. Immunol.* 2015. **15**: 630–642.

13 **Duhring, S., Germerodt, S., Skerka, C., Zipfel, P. F., Dandekar, T. and Schuster, S.**, Host-pathogen interactions between the human innate immune system and *Candida albicans*-understanding and modeling defense and evasion strategies. *Front. Microbiol.* 2015. **6**: 625.

14 **Luo, S., Skerka, C., Kurzai, O. and Zipfel, P. F.**, Complement and innate immune evasion strategies of the human pathogenic fungus *Candida albicans*. *Mol. Immunol.* 2013. **56**: 161–169.

15 **Zipfel, P. F., Skerka, C., Kupka, D. and Luo, S.**, Immune escape of the human facultative pathogenic yeast *Candida albicans*: the many faces of the Candida Pra1 protein. *Int. J. Med. Microbiol.* 2011. **301**: 423–430.

16 **Luo, S., Dasari, P., Reiher, N., Hartmann, A., Jacksch, S., Wende, E., Barz, D. et al.**, The secreted *Candida albicans* protein Pra1 disrupts host defense by broadly targeting and blocking complement C3 and C3 activation fragments. *Mol. Immunol.* 2018. **93**: 266–277.

17 **Dasari, P., Shopova, I. A., Stroe, M., Wartenberg, D., Martin-Dahse, H., Beyersdorf, N., Hortschansky, P. et al.**, Aspf2 From *Aspergillus fumigatus* recruits human immune regulators for immune evasion and cell damage. *Front. Immunol.* 2018. **9**: 1635.

18 **Funk, J., Schaarschmidt, B., Slesiona, S., Hallstrom, T., Horn, U. and Brock, M.**, The glycolytic enzyme enolase represents a plasminogen-binding protein on the surface of a wide variety of medically important fungal species. *Int. J. Med. Microbiol.* 2016. **306**: 59–68.

19 **Dasari, P., Koleci, N., Shopova, I. A., Wartenberg, D., Beyersdorf, N., Dietrich, S., Sahagun-Ruiz, A. et al.**, Enolase from *Aspergillus fumigatus* is a moonlighting protein that binds the human plasma complement proteins factor H, FHL-1, C4BP, and plasminogen. *Front. Immunol.* 2019. **10**: 2573.

20 **Pitarch, A., Nombela, C. and Gil, C.**, Serum antibody signature directed against *Candida albicans* Hsp90 and enolase detects invasive candidiasis in non-neutropenic patients. *J. Proteome Res.* 2014. **13**: 5165–5184.

21 **Chaudhary, N., Staab, J. F. and Marr, K. A.**, Healthy human T-cell responses to *Aspergillus fumigatus* antigens. *PLoS One* 2010. **5**: e9036.

22 **Knutsen, A. P. and Slavin, R. G.**, Allergic bronchopulmonary aspergillosis in asthma and cystic fibrosis. *Clin. Dev. Immunol.* 2011. **2011**: 843763.

23 **Bacher, P., Heinrich, F., Stervbo, U., Nienen, M., Vahldieck, M., Iwert, C., Vogt, K. et al.**, Regulatory T cell specificity directs tolerance versus allergy against aeroantigens in humans. *Cell* 2016. **167**: 1067–1078.e16.

24 **Bacher, P., Kniemeyer, O., Teutschbein, J., Thon, M., Vodisch, M., Wartenberg, D., Scharf, D. H. et al.**, Identification of immunogenic antigens from *Aspergillus fumigatus* by direct multiparameter characterization of specific conventional and regulatory CD4+ T cells. *J. Immunol.* 2014. **193**: 3332–3343.

25 **Bergfeld, A., Dasari, P., Werner, S., Hughes, T. R., Song, W. C., Hortschansky, P., Brakhage, A. A. et al.**, Direct binding of the pH-regulated protein 1 (Pra1) from *Candida albicans* inhibits cytokine secretion by mouse CD4+ T cells. *Front. Microbiol.* 2017. **8**: 844.

26 **Healey, D., Dianda, L., Moore, J. P., McDougal, J. S., Moore, M. J., Estess, P., Buck, D. et al.**, Novel anti-CD4 monoclonal antibodies separate human immunodeficiency virus infection and fusion of CD4+ cells from virus binding. *J. Exp. Med.* 1990. **172**: 1233–1242.

27 **Bozso, S. J., Kang, J. J. H. and Nagendran, J.**, The role of competing mechanisms on Lck regulation. *Immunol. Res.* 2020. **68**: 289–295.

28 **Giardino Torchia, M. L., Dutta, D., Mittelstadt, P. R., Guha, J., Gaida, M. M., Fish, K., Barr, V. A. et al.**, Intensity and duration of TCR signaling is limited by p38 phosphorylation of ZAP-70(T293) and destabilization of the signalosome. *Proc. Natl. Acad. Sci. USA* 2018. **115**: 2174–2179.

29 **Hardwick, J. S. and Sefton, B. M.**, Activation of the Lck tyrosine protein kinase by hydrogen peroxide requires the phosphorylation of Tyr-394. *Proc. Natl. Acad. Sci. USA* 1995. **92**: 4527–4531.

30 **Hardwick, J. S. and Sefton, B. M.**, The activated form of the Lck tyrosine protein kinase in cells exposed to hydrogen peroxide is phosphorylated at both Tyr-394 and Tyr-505. *J. Biol. Chem.* 1997. **272**: 25429–25432.

31 **Vaz, C., Pitarch, A., Gomez-Molero, E., Amador-Garcia, A., Weig, M., Bader, O., Monteoliva, L. et al.**, Mass spectrometry-based proteomic and immunoproteomic analyses of the *Candida albicans* hyphal secretome reveal diagnostic biomarker candidates for invasive candidiasis. *J. Fungi (Basel)* 2021. **7**: 501.

32 **Sueyoshi, K., Ledderose, C., Shen, Y., Lee, A. H., Shapiro, N. I. and Junger, W. G.**, Lipopolysaccharide suppresses T cells by generating extracellular ATP that impairs their mitochondrial function via P2Y11 receptors. *J. Biol. Chem.* 2019. **294**: 6283–6293.

33 **Martinez, R. J., Andargachew, R., Martinez, H. A. and Evavold, B. D.**, Low-affinity CD4+ T cells are major responders in the primary immune response. *Nat. Commun.* 2016. **7**: 13848.

34 **von Lilienfeld-Toal, M., Wagener, J., Einsele, H., Cornely, O. A. and Kurzai, O.**, Invasive fungal infection. *Dtsch. Arztebl. Int.* 2019. **116**: 271–278.

35 **Brown, G. D., Denning, D. W., Gow, N. A., Levitz, S. M., Netea, M. G. and White, T. C.**, Hidden killers: human fungal infections. *Sci. Transl. Med.* 2012. **4**: 165rv113.

36 **Stuehler, C., Khanna, N., Bozza, S., Zelante, T., Moretti, S., Kruhm, M., Lurati, S. et al.**, Cross-protective TH1 immunity against *Aspergillus fumigatus* and *Candida albicans*. *Blood* 2011. **117**: 5881–5891.

37 **Konig, M., Rharbaoui, F., Aigner, S., Dalken, B. and Schuttrumpf, J.**, Tregalizumab – a monoclonal antibody to target regulatory T cells. *Front. Immunol.* 2016. **7**: 11.

38 **Chen, W., Feng, Y., Gong, R., Zhu, Z., Wang, Y., Zhao, Q. and Dimitrov, D. S.**, Engineered single human CD4 domains as potent HIV-1 inhibitors and components of vaccine immunogens. *J. Virol.* 2011. **85**: 9395–9405.

39 **Hester, R. A. and Kennedy, S. B.**, Candida infection as a risk factor for HIV transmission. *J. Womens Health (Larchmt)* 2003. **12**: 487–494.

40 **Ricciardi, S., Manfrini, N., Alfieri, R., Calamita, P., Crosti, M. C., Gallo, S., Muller, R. et al.**, The translational machinery of human CD4(+) T cells is poised for activation and controls the switch from quiescence to metabolic remodeling. *Cell Metab.* 2018. **28**: 961.

41 **Chang, C. H., Curtis, J. D., Maggi, L. B., Jr., Faubert, B., Villarino, A. V., O'Sullivan, D., Huang, S. C. et al.**, Posttranscriptional control of T cell effector function by aerobic glycolysis. *Cell* 2013. **153**: 1239–1251.

42 **Langenhorst, D., Furst, A. L., Alberter, K., Vilhena, C., Dasari, P., Daud, M., Heilig, L. et al.**, Soluble Enolase 1 of *Candida albicans* and *Aspergillus fumi-*

gatus stimulates human and mouse B Cells and monocytes. *J. Immunol.* 2023: ji2200318.

43 **Aozasa, M., Amino, N., Iwatani, Y., Tamaki, H., Watanabe, Y., Sato, H., Hochito, K. et al.**, Familial OKT4 epitope deficiency: studies on antigen density and lymphocyte function. *Clin. Immunol. Immunopathol.* 1985. **37**: 48–55.

44 **Fukuda, T., Matsunaga, M., Kurata, A., Mine, M., Ikari, N., Katamine, S., Kanazawa, H. et al.**, Hereditary deficiency of OKT4-positive cells: studies for mode of inheritance and lymphocyte functions. *Immunology* 1984. **53**: 643–649.

45 **Hughes, E. J., Goddard, E. A., Bouic, P. and Beatty, D. W.**, Flow cytometry analysis of OKT4 epitope deficiency in South African black children. *Clin. Exp. Immunol.* 1994. **98**: 526–531.

46 **Mayer, C. T., Huntenburg, J., Nandan, A., Schmitt, E., Czeloth, N. and Sparwasser, T.**, CD4 blockade directly inhibits mouse and human CD4(+) T cell functions independent of Foxp3(+) Tregs. *J. Autoimmun.* 2013. **47**: 73–82.

47 **Bacher, P., Rosati, E., Esser, D., Martini, G. R., Saggau, C., Schiminsky, E., Dargvainiene, J. et al.**, Low-avidity CD4(+) T cell responses to SARS-CoV-2 in unexposed individuals and humans with severe COVID-19. *Immunity* 2020. **53**: 1258–1271.e5.

48 **Diaz-Ramos, A., Roig-Borrellas, A., Garcia-Melero, A. and Lopez-Alemany, R.**, alpha-Enolase, a multifunctional protein: its role on pathophysiological situations. *J. Biomed. Biotechnol.* 2012. **2012**: 156795.

49 **Bedke, T., Iannitti, R. G., De Luca, A., Giovannini, G., Fallarino, F., Berges, C., Latge, J. P. et al.**, Distinct and complementary roles for *Aspergillus fumigatus*-specific Tr1 and Foxp3+ regulatory T cells in humans and mice. *Immunol. Cell Biol.* 2014. **92**: 659–670.

Abbreviations: **CaEno1**: *Candida albicans* Eno1 · **CFSE**: carboxyfluorescein succinimidyl ester · **HLA**: human leukocyte antigen · **IFD**: invasive fungal disease · **mAb**: monoclonal antibodies · **PBMC**: peripheral blood mononuclear cell · **PPD**: purified protein derivative · **TCR**: T-cell receptor

Full correspondence: Dr. Niklas Beyersdorf, Institute for Virology and Immunobiology, Versbacher Str. 7, D-97078 Würzburg, Germany
e-mail: niklas.beyersdorf@vim.uni-wuerzburg.de

Received: 23/11/2022
Revised: 5/6/2023
Accepted: 27/7/2023
Accepted article online: 28/7/2023